

2
3
4 **A promising new baseflow method and recession**
5 **approach for streamflow at Glendhu Catchment, New**
6 **Zealand**

7
8
9
10 **M. K. Stewart¹**

11
12 ¹Aquifer Dynamics & GNS Science, PO Box 30368, Lower Hutt 5040, New Zealand

13
14 Correspondence to: M.K. Stewart (m.stewart@gns.cri.nz)

15
16

17 **Abstract**

18

19 Understanding and modelling the relationship between rainfall and runoff has been a
20 driving force in hydrology for many years. Baseflow separation and recession analysis
21 have been two of the main tools for understanding runoff generation in catchments, but
22 there are many different methods for each. The new baseflow separation method
23 presented here (the bump and rise method or BRM) aims to accurately simulate the shape
24 of tracer-determined baseflow or pre-event water. Application of the method by
25 calibrating its parameters, using (a) tracer data or (b) an optimizing method, is
26 demonstrated for the Glendhu Catchment, New Zealand. The calibrated BRM algorithm
27 is then applied to the Glendhu streamflow record. The new recession approach advances
28 the thesis that recession analysis of streamflow alone gives misleading information on
29 catchment storage reservoirs because streamflow is a varying mixture of components of
30 very different origins and characteristics (at the simplest level, quickflow and baseflow as
31 identified by the BRM method). Recession analyses of quickflow, baseflow and
32 streamflow show that the steep power-law slopes often observed for streamflow at
33 intermediate flows are artifacts due to such mixing and are not representative of
34 catchment reservoirs. Applying baseflow separation before recession analysis could
35 therefore shed new light on water storage reservoirs in catchments and possibly resolve
36 some current problems with recession analysis. Among other things it shows that both
37 quickflow and baseflow reservoirs in the studied catchment have (non-linear) quadratic
38 characteristics.

39

40 1 Introduction

41

42 Interpretation of streamflow variations in terms of catchment characteristics has been a
43 major theme in hydrology for many years in order to improve catchment and stream
44 management. Two of the main tools for this task are baseflow separation and recession
45 analysis (Hall, 1968; Brutsaert and Nieber, 1977; Tallaksen, 1995; Smakhtin, 2001).
46 Baseflow separation aims to separate streamflow into two components (quickflow and
47 baseflow), where quickflow is direct runoff following rainfall, and baseflow is delayed
48 streamflow during periods without rain. Recession analysis aims to model the decrease of
49 streamflow during rainless periods to extract parameters descriptive of water storage in
50 the catchment. In a similar way, transit time analysis determines transit time distributions
51 of water in the stream and catchment in order to quantify flowpaths and storages through
52 the catchment. To fully understand and satisfactorily model the movement of water and
53 chemicals through catchments, it is necessary to understand in detail the water stores and
54 flowpaths (Fenicia et al., 2011; McMillan et al., 2011; Beven et al., 2012; Hrachowitz et
55 al., 2013).

56

57 The technique of baseflow separation has a long history in practical and scientific
58 hydrology because knowledge about baseflow is very useful in predicting low flow
59 progressions and understanding water quality variations. Although considered to some
60 extent arbitrary by some (e.g. Hewlett and Hibbert, 1967; Beven, 1991), most of the
61 methods yield results that are quite similar (e.g. Gonzales et al., 2009 obtained long-term
62 baseflow fractions (i.e. baseflow indexes, called BFIs below) ranging from 0.76 to 0.91
63 for nine non-tracer baseflow separation methods, not too different from their tracer-based
64 result of 0.90), and all show that baseflow is often quantitatively important in annual
65 flows and, of course, very important during low flows. This work contends that baseflow
66 should also be specifically considered during intermediate and high flows, because
67 streamflow during such events is composed of comparable amounts of both quickflow
68 and baseflow (e.g. Sklash and Farvolden, 1979) and they are produced by very different
69 mechanisms. Consequently, it is believed that process descriptors such as hydrograph
70 recession constants (or transit time distribution parameters) should be determined on
71 separated components as well as total streamflow during such flows, because streamflow
72 is a mixture and therefore can give misleading results. All such process descriptors
73 should be qualified by the components they were derived from. Putting it simply, the
74 contention is that to properly understand the early streamflow recession hydrograph it is
75 first necessary to separate it into its quickflow and baseflow components. While this may
76 be considered obvious by some, recession analysis has not previously been applied to
77 other than the total streamflow.

78

79 Recession analysis also has a long history for practical hydrology reasons, but Stoelzle et
80 al. (2013) recently highlighted large discrepancies between different methods of analysis,
81 in particular contrasting recession parameters derived by the methods of Brutsaert and
82 Nieber (1977), Vogel and Kroll (1992), and Kirchner (2009). Stoelzle et al. suggested
83 that “a multiple methods approach to investigate streamflow recession characteristics
84 should be considered”. This indicates that there is little general consensus on how best to
85 apply recession analysis to streamflow.

86

87 This paper presents a new method of baseflow separation (called the bump and rise
88 method or BRM) which aims to accurately simulate the shape of tracer-determined
89 baseflow or pre-event water. The two BRM parameters are calibrated by (a) fitting to

90 tracer data if it is available, or (b) using an optimizing process if it is not. The calibrated
91 BRM filter is then applied to the streamflow record. Two other baseflow separation
92 methods (those of Hewlett and Hibbert (1967) and Eckhardt (2005)) are compared with
93 the BRM. The paper also takes a fresh look at the application of recession analysis for
94 characterising runoff generation processes. Recession analysis of streamflow can give
95 misleading slopes on a recession plot particularly at intermediate flows because
96 streamflow is a varying mixture of components (at the simplest level, quickflow and
97 baseflow). When quickflow, baseflow and streamflow are all analysed, the effect of the
98 more rapidly receding quickflow on the streamflow can be seen. The same procedure
99 gives insight into the processes of streamflow generation at each exceedence percentage
100 when applied to flow duration curves (Section 2.4). The methods are illustrated using
101 streamflow data from the Glendhu Catchment in Otago, South Island, New Zealand.

102
103

104 **2 Methods and Study Site**

105

106 **2.1 Baseflow Separation**

107

108 Justification for making baseflow separations rests on the dissimilarity of quickflow and
109 baseflow generation processes in catchments (e.g. Hewlett and Hibbert, 1967). Evidence
110 of this is given by the different recession slopes, and chemical and stable isotope
111 compositions of early and late recessions in hydrographs (examples are given for
112 Glendhu, see below). In addition, transit times of stream water show great differences
113 between quickflow and baseflow. While quickflow is young (as shown by the variations
114 of conservative tracers and radioactive decay of tritium), baseflow can be much older
115 with substantial fractions of water having mean transit times beyond the reach of
116 conservative tracer variations (4 years) and averaging 10 years as shown by tritium
117 measurements (Stewart et al., 2010, 2012; Michel et al., 2014). For these reasons, it is
118 believed that it is not justifiable to treat the streamflow as a single component, but that at
119 least two components should be considered by applying baseflow separation to the
120 hydrograph before analysis.

121

122 Streamflow at any time (Q_t) is composed of the sum of quickflow (A_t) and baseflow (B_t)

123

$$124 \quad Q_t = A_t + B_t \quad (1)$$

125

126 where time steps are indicated by the sequences ... Q_{t-1} , Q_t , Q_{t+1} ... etc. The time
127 increment is one hour in the examples given below, but can be days in larger catchments
128 or any regular interval. Quickflow or direct runoff results from rainfall events and often
129 drops to zero between events, while baseflow is continuous as long as the stream flows.
130 As shown by the names, the important distinction between them is the time of release of
131 water particles to the stream (i.e. their transit times through the catchment). They are
132 supplied by fast and slow drainages within the catchment, direct precipitation and fast
133 storage reservoirs (soil stores) supply quickflow, and slow storage reservoirs (mainly
134 groundwater aquifers) supply baseflow. This simple separation has proven to be effective
135 in many catchments, and is practical for the general case considered here. However,
136 particular catchments may have a variety of different possible streamflow components
137 that could be separated in principle. Fig. 1 gives a recession curve as an example showing
138 schematically the two flow components and the early and late parts of the curve. The late

139 part of the recession curve starts when baseflow dominates streamflow (i.e. quickflow
140 becomes very small).

141

142 Many methods have been developed for baseflow separation (see reviews by Hall, 1968;
143 Tallaksen, 1995; Gonzales et al., 2009). Baseflow separation methods can be grouped
144 into three categories: analytical, empirical and chemical/isotopic or tracer methods.

145 Analytical methods are based on fundamental theories of groundwater and surface water
146 flows. Examples are the analytical solution of the Boussinesq equation, the unit
147 hydrograph model and theories for reservoir yields from aquifers (Boussinesq, 1877; Su,
148 1995; Nejadhashemi et al., 2003). Empirical methods based on the hydrograph are the
149 most widely used (Zhang et al., 2013), because of the availability of such data. The
150 methods include 1) recession analysis (Linsley et al., 1975), 2) graphical methods,
151 filtering streamflow data by various methods (e.g. finding minima within predefined
152 intervals and connecting them) (e.g. Sloto and Crouse, 1996), 3) low pass filtering of the
153 hydrograph (Eckhardt, 2005; Zhang et al., 2013), and 4) using groundwater levels to
154 calculate baseflow contributions based on previously determined relationships between
155 groundwater levels and streamflows (Holko et al., 2002).

156

157 One widely-used empirical method for small catchments was proposed by Hewlett and
158 Hibbert (1967) who argued that: “since an arbitrary separation must be made in any case,
159 why not base the classification on a single arbitrary decision, such as a fixed, universal
160 method for separating hydrographs on all small watersheds?” They separated the
161 hydrograph into “quickflow” and “delayed flow” components by arbitrarily projecting a
162 line of constant slope from the beginning of any stream rise until it intersected the falling
163 side of the hydrograph. The steady rise is described by the equations

164

$$165 \quad B_t = B_{t-1} + k \quad \text{for} \quad Q_t > B_{t-1} + k \quad (2)$$

$$166 \quad B_t = Q_t \quad \text{for} \quad Q_t \leq B_{t-1} + k \quad (3)$$

167

168 where k is the slope of the dividing line. The slope they chose was $0.05 \text{ ft}^3/\text{sec}/\text{mile}^2/\text{hour}$
169 ($0.000546 \text{ m}^3/\text{s}/\text{km}^2/\text{h}$ or $0.0472 \text{ mm}/\text{d}/\text{h}$). This universal slope gives a firm basis for
170 comparison of BFIs between catchments.

171

172 Tracer methods use dissolved chemicals and/or stable isotopes to separate the hydrograph
173 into component hydrographs based on mass balance of water and tracers. Waters from
174 different sources are assumed to have unique and constant (or varying in a well-
175 understood way) compositions (Pinder and Jones, 1969; Sklash and Farvolden, 1979;
176 McDonnell et al., 1991). These tracer methods allow objective separation of the
177 hydrograph, but it is important to consider just what water components are being
178 separated. For example, deuterium varies much more in rainfall than it does in soil or
179 groundwater, which has average deuterium concentrations from contributions from
180 several past events. When the deuterium content of a particular rainfall is very high or
181 very low, it becomes an effective indicator of the presence of “event” water in the stream,
182 compared with the “pre-event” water already in the catchment before rainfall began (as
183 shown in Fig. 2a adapted from Bonell et al., 1990). Baseflow separations (i.e.
184 identification of a groundwater component) have been more specifically shown by three-
185 component separations using chemicals and stable isotopes (Bazemore et al., 1994;
186 Hangin et al., 2001; Joerin et al., 2002; Iwagami et al., 2010). An example of separation
187 of direct precipitation, acid soil and groundwater components using silica and calcium is
188 given in Fig. 2b redrawn from Iorgulescu et al. (2005).

189

190 A remarkable and by now well-accepted characteristic of these separations is that the
191 components including groundwater often respond to rainfall as rapidly as the stream
192 itself. Chapman and Maxwell (1996) noted that “hydrograph separation using tracers
193 typically shows a highly responsive old flow”. Likewise Wittenberg (1999) comments
194 “tracers such as ^{18}O ... and salt ... [show] that even in flood periods outflow from the
195 shallow groundwater is the major contributor to streamflow in many hydrological
196 regimes”. And Klaus and McDonnell (2013) observe “most [tracer studies] showed a
197 large preponderance of pre-event water in the storm hydrograph, even at peak flow”. This
198 has been a general feature in tracer studies and includes all of the components tested
199 whether quickflow or baseflow (e.g. Hooper and Shoemaker, 1986; Bonell et al., 1990;
200 Buttle, 1994; Gonzales et al., 2009; Zhang et al., 2013). In the case of groundwater, the
201 rapid response is believed to be partially due to rapid propagation of rainfall effects
202 downwards (by pressure waves or celerity) causing rapid water table rise and
203 displacement of stored water near the stream (e.g. Beven, 2012, page 349; McDonnell
204 and Beven, 2014; Stewart et al., 2007, page 3354).

205

206 Chapman and Maxwell (1996) and Chapman (1999) compared baseflow separations
207 based on digital filters (like the low pass filters referred to above) with tracer separations
208 in the literature and identified a preferred two-parameter algorithm given by

209

$$210 \quad B_t = \frac{m}{1+C} B_{t-1} + \frac{C}{1+C} Q_t \quad (4)$$

211

212 which approximately matched the tracer separations. m and C are parameters identified
213 by fitting to the pre-event hydrograph identified by tracers. Eckhardt (2005)
214 demonstrated that some previously published digital filters (Lyne and Hollick, 1979;
215 Chapman and Maxwell, 1996; Chapman, 1999) could be represented by a more general
216 digital filter equation by assuming a linear relationship between baseflow and baseflow
217 storage (see equation 9 below). Eckhardt’s filter is

218

$$219 \quad B_t = \frac{(1-BFI_{max})aB_{t-1} + (1-a)BFI_{max}Q_t}{1-aBFI_{max}} \quad (5)$$

220

221 where parameter a is a recession constant relating adjacent baseflow steps during
222 recessions, i.e.

223

$$224 \quad B_t = aB_{t-1} \quad (6)$$

225

226 and is determined by recession analysis. On the other hand, there was no objective way to
227 determine parameter BFI_{max} (the maximum value of the baseflow index that can be
228 modeled by the algorithm corresponding to low-pass filtering of a wave of infinite
229 length). Eckhardt (2005) suggested that typical BFI_{max} values can be found for classes of
230 catchments based on their hydrological and hydrogeological characteristics (e.g. 0.8 for
231 perennial streams in catchments with permeable bedrock). Others have pointed out that
232 these BFI_{max} values should be regarded as first approximations, and more refined values
233 can be determined using tracers (Eckhardt, 2008; Gonzales et al., 2009; Zhang et al.,
234 2013), by a backwards filtering operation (Collischonn and Fan, 2013) or by the
235 relationship of two characteristic values from flow duration curves (i.e. Q_{90}/Q_{50} ,
236 Smakhtin, 2001; Collischonn and Fan, 2013).

237

2.1.1 The new baseflow separation method

238
239

240 The new baseflow separation method put forward in this paper (hereafter called the bump
241 and rise method or BRM) has an algorithm chosen to simulate tracer separations simply
242 but accurately. Tracer separations show rapid baseflow responses to storm events (the
243 “bump”), which is followed in the method by a steady rise in the sense of Hewlett and
244 Hibbert (1967) (the “rise”). The steady rise is justified by increase in catchment wetness
245 conditions and gradual replenishment of groundwater aquifers during rainy periods. The
246 size of the bump (f) and the slope of the rise (k) are parameters of the recursive digital
247 filter that can be applied to the streamflow record. The separation procedure is described
248 by the equations:

249

$$250 \quad B_t = B_{t-1} + k + f(Q_t - Q_{t-1}) \quad \text{for} \quad Q_t > B_{t-1} + k \quad (7)$$

$$251 \quad B_t = Q_t \quad \text{for} \quad Q_t \leq B_{t-1} + k \quad (8)$$

252

253 where f is a constant fraction of the increase or decrease of streamflow during an event.
254 The values of f and k can be determined from tracer measurements, like the parameters of
255 other digital filters. If no tracer information is available, f and k can be determined by an
256 optimization process as described in an earlier version of this paper (Stewart, 2014a). A
257 particular feature of the BRM method is that two types of baseflow response are included,
258 a short-term response via the bump and a longer-term response via the rise.

259

2.2 Recession Analysis

260
261

262 Recession analysis also has a long history. Stoelzle (2013) recently highlighted
263 discrepancies between methods of extracting recession parameters from empirical data by
264 contrasting results from three established methods (Brutsaert and Nieber, 1977, Vogel
265 and Kroll, 1992, and Kirchner, 2009). They questioned whether such parameters are
266 really able to characterise catchments to assist modelling and regionalisation, and
267 suggested that researchers should use more than one method because specific catchment
268 characteristics derived by the different recession analysis methods were so different.

269

270 The issue of whether storages can be represented by linear reservoirs or require to be
271 treated as non-linear reservoirs has been widely discussed in the hydrological literature
272 (in the case of recession analysis by Brutsaert and Nieber, 1977, Tallaksen, 1995, Lamb
273 and Beven, 1997 and Fenicia et al., 2006, among others). Lamb and Beven (1997)
274 identified three different storage behaviours in the three catchments they studied. Linear
275 reservoirs only require one parameter each and are more tractable mathematically. They
276 are widely used in rainfall-runoff models. Non-linearity can be approximately
277 accommodated by using two or more linear reservoirs in parallel, but more parameters
278 are required (three in the case of two reservoirs). Linear storage is expressed by the
279 formulation

280

$$281 \quad V = Q/\beta \quad (9)$$

282

283 where V is storage volume, and β is a constant (with dimensions of T^{-1}). The exponential
284 relationship follows for baseflow recessions

285

$$286 \quad Q_t = Q_o \exp(-\beta t) \quad (10)$$

287

288 where Q_0 is the streamflow at the beginning of the recession.

289

290 However, evidence for non-linearity is strong (Wittenberg, 1999) and the non-linear
291 formulation is often used

292

$$293 \quad V = eQ^b \quad (11)$$

294

295 where e and b are constants. This gives the recession equation

296

$$297 \quad Q_t = Q_0 \left[1 + \frac{(1-b)Q_0^{(1-b)}}{eb} t \right]^{1/(b-1)} \quad (12)$$

298

299 The exponent b has been found to take various values between 0 and 1.1, with an average
300 close to 0.5 (Wittenberg, 1999). $b=1$ gives the linear storage model (equations 8 and 9).

301 For $b=0.5$, equation 11 reduces to the quadratic equation

302

$$303 \quad Q_t = Q_0 \left[1 + \frac{1}{e} \cdot Q_0^{0.5} \cdot t \right]^{-2} \quad (13)$$

304

305 This quadratic equation is similar to the equation derived much earlier by Boussinesq
306 (1903) as an analytical solution for drainage of a homogeneous groundwater aquifer
307 limited by an impermeable horizontal layer at the level of the outlet to the stream

308

$$309 \quad Q_t = Q_0(1 + \alpha t)^{-2} \quad (14)$$

310

311 where α is

312

$$313 \quad \alpha = KB/PL^2 \quad (15)$$

314

315 Here K is the hydraulic conductivity, P the effective porosity, B the effective aquifer
316 thickness, and L the length of the flow path. Dewandel et al. (2003) have commented that
317 only this quadratic form is likely to give correct values for the aquifer properties because
318 it is an exact analytical solution to the diffusion equation, albeit with simplifying
319 assumptions, whereas other forms (e.g. exponential) are approximations.

320

321 In order to generalise recession analysis for a stream (i.e. to be able to analyse the
322 stream's recessions collectively rather than individually) Brutsaert and Nieber (1977)
323 presented a method based on the power-law storage-outflow model, which describes flow
324 from an unconfined aquifer into a stream. The negative gradient of the discharge (i.e. the
325 slope of the recession curve) is plotted against the discharge, thereby eliminating time as
326 a reference. This is called a recession plot below (following Kirchner, 2009). To keep the
327 timing right, the method pairs streamflow $Q = (Q_{t-1} + Q_t)/2$ with negative streamflow
328 recession rate $-dQ/dt = Q_t - Q_{t-1}$.

329

330 Change of storage in the catchment is given by the water balance equation:

331

$$332 \quad \frac{dV}{dt} = R - E - Q \quad (16)$$

333

334 where R is rainfall and E is evapotranspiration. Assuming no recharge or extraction, we
335 have

336

337

$$\frac{dV}{dt} = -Q \quad (17)$$

338

339 from whence equation 10 leads to

340

341

$$-\frac{dQ}{dt} = \frac{1}{eb} Q^{2-b} = cQ^d \quad (18)$$

342

343 The exponent d allows for both linear ($d=1$) and non-linear ($d \neq 1$) storage outflow
344 relationships, with $d=1.5$ giving the frequently observed quadratic relationship (equation
345 12). Authors who have investigated the dependence of $-dQ/dt$ on Q for late recessions
346 (low flows) have often found d averaging close to 1.5 (e.g. Brutsaert and Nieber, 1977;
347 Wittenberg, 1999; Dewandel, 2005; Stoelzle et al., 2013). Higher values of d were often
348 found especially at higher flows, e.g. Brutsaert and Nieber (1977) found values of $d = 3$
349 for the early parts of recessions.

350

351 Recent work has continued to explore the application and possible shortcomings of the
352 recession plot method. Rupp and Selker (2006) proposed scaling of the time increment to
353 the flow increment which can greatly reduce noise and artifacts in the low-flow part of
354 the plot. Biswal and Marani (2010) identified a link between recession curve properties
355 and river network morphology. They found slopes of individual recession events in
356 recession plots (d values) averaging around 2 and ranging from 1.1 to 5.5. In a small (1
357 km^2) catchment, McMillan et al. (2011) showed that individual recessions plotted on the
358 recession plot “shifted horizontally with season”, which they attributed to changes in
359 contributing subsurface reservoirs as streamflow levels changed with season. This
360 explanation is analogous to the approach below in that two water components with
361 different storage characteristics are implied. The slopes of individual recessions in their
362 analysis were in excess of 2 with the low-flow tails being very much steeper. In medium
363 to large catchments (100 - 6,414 km^2), Shaw and Riha (2012) found curves of individual
364 recessions “shifted upwards in summer relative to early spring and late fall curves”,
365 producing a data cloud when recessions from all seasons were combined. They speculate
366 that the movement with season (which was similar, but less extreme to that seen by
367 McMillan et al., 2011 above) was due to seasonal changes of catchment
368 evapotranspiration. They found that the slopes of individual recessions were often close
369 to 2 and had an extreme range of 1.3 to 5.3.

370

371 Problems in determining recession parameter values from streamflow data on recession
372 plots are due to 1) different recession extraction methods (e.g. different selection criteria
373 for data points), and 2) different parameter-fitting methods to the power-law storage-
374 outflow model (equation 17). There is generally a very broad scatter of points on the
375 plots, which makes parameter-fitting difficult. Clearly evapotranspiration is likely to play
376 a role in producing some of the scatter because evapotranspiration was neglected from
377 equation 16. However, it is also believed that part of the scatter is due to recession
378 analysis being applied to streamflow rather than to its separated components (see below).

379

380 **2.2.1 The New Recession Analysis Approach**

381

382 The new approach proposed here consists of applying recession analysis via the recession
383 plot to separated quickflow and baseflow components as well as to the streamflow. The
384 rationale for this is that quickflow and baseflow derive from different storages within the

385 catchment. In particular, the changing proportions of quickflow and baseflow in
386 streamflow during early parts of recessions cause recession analyses of streamflow to
387 give mixed messages, i.e. misleading results not characteristic of storages in the
388 catchment, as demonstrated for Glendhu Catchment below. This is expected to have led
389 to some previous recession analysis studies giving misleading results in regard to
390 catchment storage in cases where early recession streamflow has been analysed.

391 **2.3 Flow Duration Curves**

392
393
394 Flow duration curves (FDCs) represent in one figure the flow characteristics of a stream
395 throughout its range of variation. They are cumulative frequency curves that show the
396 percentages of time during which specified discharges were equalled or exceeded in
397 given periods. They are useful for practical hydrology (Searcy, 1959), and have been
398 used as calibration targets for hydrologic models (Westerberg et al., 2011).

399
400 FDCs can also be determined for the separated stream components as shown below (Fig.
401 5d). Although FDCs for streamflow are not misleading and obviously useful in their own
402 right, FDCs of separated components can give insight into the processes of streamflow
403 generation at each exceedence percentage.

404 **2.4 Hydrogeology of Glendhu Catchment**

405
406
407 GH1 catchment (2.18 km²) is situated 50 km inland from Dunedin in the South Island of
408 New Zealand. It displays rolling-to-steep topography and elevation ranges from 460 to
409 650 m.a.s.l. (Fig. 3). Bedrock is moderately-to-strongly weathered schist, with the
410 weathered material filling in pre-existing gullies and depressions. Much of the bedrock-
411 colluvial surface is overlain by a loess mantle of variable thickness (0.5 to 3 m). Well-to-
412 poorly drained silt loams are found on the broad interfluvies and steep side slopes, and
413 poorly drained peaty soils in the valley bottoms.

414
415 Amphitheatre-like sub-catchments are common features in the headwaters and frequently
416 exhibit central wetlands that extend downstream as riparian bogs. Snow tussock
417 (*Chionochloa rigida*) is the dominant vegetation cover and headwater wetlands have a
418 mixed cover of sphagnum moss, tussock, and wire grass (*Empodisma minus*). The mean
419 annual temperature within GH1 at 625 m.a.s.l. elevation is 7.6C, and the mean annual
420 rainfall is 1350 mm/a. Annual runoff is measured at all weirs to an accuracy of $\pm 5\%$
421 (Pearce et al., 1984).

422
423 Pearce et al. (1984) showed that GH1 and GH2 (before the latter was forested), had very
424 similar runoff ratios. Long term precipitation and runoff at GH1 weir average 1350 mm/a
425 and 743 mm/a respectively (Fahey and Jackson, 1997). Actual evapotranspiration of 622
426 mm/a was measured for tussock grassland in the period April 1985 to March 1986 at a
427 nearby site in catchment GH1 (570 m a.s.l.) by Campbell and Murray (1990) using a
428 weighing lysimeter. The Priestley-Taylor estimate of PET was 643 mm/a for the period,
429 and 599 mm/a for 1996, so ET for GH1 is taken as 600 mm/a. The GH1 hydrological
430 balance is: Precipitation (1350 mm/a) – ET (600 mm/a) = Runoff (743 mm/a), and loss
431 around the weir is clearly negligible (Pearce et al. 1984). Comparison of runoff from
432 GH1 and GH2 (after the latter had been forested for 7 years), showed that there was a
433 decrease of 260 mm/a in GH2 runoff due to afforestation (Fahey and Jackson, 1997).
434 Consequently, the GH2 balance is: Precipitation (1350 mm/a) – ET (860 mm/a) = Runoff

435 (483 mm/a). The increase in ET for GH2 is attributed to increased interception (with
436 evaporative loss) and transpiration.

437

438 Bonell et al. (1990) carried out separation of event and pre-event waters using deuterium
439 and chloride concentrations to investigate the runoff mechanisms operating in GH1 and
440 GH2 at Glendhu (see example in Fig. 2a). The results showed that for quickflow volumes
441 greater than 10 mm (over the catchment area), the early part of the storm hydrograph
442 could be separated into two components, pre-event water from a shallow unconfined
443 groundwater aquifer, and event water attributed to “saturated overland flow”. The pre-
444 event water responded more rapidly to rainfall than event water. The late part of the
445 storm hydrograph consisted of pre-event water only. Hydrographs for smaller storms had
446 pre-event water only, but this may be partly because measurement accuracy of the
447 deuterium may not have been sufficient to detect event water in these smaller events.

448

449 **3 Results of Application of New Approaches to Glendhu GH1** 450 **Catchment**

451

452 The BRM baseflow separation method is applied to Glendhu GH1 catchment to
453 investigate its applicability, demonstrate how it is applied and present what it reveals
454 about the catchment. The results are compared with those from two other widely-used
455 baseflow separation filters, the Hewlett and Hibbert (1965) method (called the H & H
456 method below) and the Eckhardt (2005) method (called the Eckhardt method). We need
457 to know the values of the parameters of these methods in order to apply them, the
458 parameters are k (the universal slope of the rise through the event) for the H & H method,
459 BFI_{max} (the maximum value of the baseflow index that can be modeled by the Eckhardt
460 algorithm) and a (recession constant) for the Eckhardt method, and f (bump fraction) and
461 k (slope of the rise) for the BRM method.

462

463 The parameter k for the H & H method has the universal (arbitrary) value of 0.0472 mmd^{-1}
464 h^{-1} , as explained above. Estimation of the Eckhardt parameters is not so simple (see
465 above) and has similarities to the estimation of the BRM parameters. There are two ways
466 of determining the Eckhardt and BRM parameters: (1) By adjusting the baseflow
467 parameters to give the best fits between the baseflows and the tracer-determined pre-
468 event or baseflow water. This is regarded as the only objective way, and is able to be used
469 in this paper because deuterium data is available for Glendhu (Bonell et al., 1990). But it
470 requires tracer data during events which is not generally available for catchments. (2)
471 Where there is no tracer data, the parameters can be estimated in several ways. In the
472 prescribed Eckhardt method, a is calculated from the late part of the recession by an
473 objective procedure. BFI_{max} is estimated to a first approximation based on the
474 hydrological and hydrogeological characteristics of the catchment (Eckhardt (2005), and
475 possibly more precisely by hydrograph methods suggested by Collischonn and Fan
476 (2013) (see Section 3.1). For the BRM, the BFI can be estimated approximately from
477 catchment considerations (in analogy with the Eckhardt method) and possibly more
478 precisely by a flow duration curve method suggested by Collischonn and Fan (2013). The
479 BFI can then be used as a constraint while optimising the fit between the sum and the
480 streamflow (where the sum equals the baseflow plus a fast recession). This optimising
481 procedure was used in the earlier version of this paper (Stewart, 2014a). The optimising
482 procedure was also applied to the H & H and Eckhardt methods in the Author’s Reply
483 (Stewart, 2014b).

484

485 Once baseflow separation has been achieved, recession analysis via the recession plot can
486 be applied to the separated quickflow and baseflow components (the new approach
487 suggested here), in addition to the streamflow (the traditional method). Whereas the
488 streamflow can show high power law slopes (d values of 2 or more), the components
489 generally have slopes around 1.5. However, note that in the early part of the recession the
490 baseflow is a subdued reflection of the streamflow because of its calculation procedure
491 (equations 6 and 7), while in the late part of the recession the baseflow and the
492 streamflow are the same. Flow duration curve analysis can also be applied to the
493 components as well as to the streamflow in order to show the makeup of the streamflow
494 at each exceedence percentage.

495

496 **3.1 Application of Baseflow Separation Methods**

497

498 Fig. 2a showed the pre-event component determined using deuterium during the large
499 storm on 23 February 1988 (Bonell et al., 1990). The pre-event component has a BFI of
500 0.529 during the event (Table 1). Baseflows determined by the three baseflow separation
501 methods are compared with the pre-event component in Figs. 4a-c. The goodness of fit of
502 the baseflows to the pre-event water was determined using least squares,

503

$$504 \quad sd = (\sum(B_i - PE_i)^2 / N)^{0.5} \quad (19)$$

505

506 where PE_i is the pre-event water at each time step, and N the number of values. The H &
507 H baseflow is totally inflexible with a pre-determined parameter and does not match the
508 BFI or shape of the pre-event hydrograph at all well (its BFI is 0.255 and sd is 6.41
509 mm/d, Table 1, Fig. 4a).

510

511 The Eckhardt baseflow with prescribed parameters ($BFI_{max} = 0.8$ for a porous perennial
512 stream, $a = 0.99817$ calculated from the baseflow recession) does not match the pre-event
513 hydrograph well either ($BFI = 0.272$, $sd = 6.34$ mm/d, Fig. 4c). However, a better match
514 of the BFI and a slightly better fit is found with the optimized version when both BFI_{max}
515 and a are treated as adjustable parameters using the method of Zhang et al., 2013 (i.e.
516 BFI_{max} was adjusted first to match the Eckhardt BFI to the pre-event BFI, then a was
517 adjusted to improve the fit between the shapes of the baseflow and the pre-event
518 hydrographs, then the steps were repeated, etc.). An extra constraint was to prevent the
519 Eckhardt baseflow falling too far below the streamflow at very low flows. These give a
520 BFI of 0.524, which is the same as that of the pre-event hydrograph (0.529, Table 1), and
521 the baseflow has a similar shape to the pre-event water (Fig. 4c), but the peak is delayed
522 in time giving only a small improvement in the fit ($sd = 5.40$ mm/d).

523

524 The BRM baseflow gives a BFI of 0.526, the same as that of the pre-event hydrograph,
525 and the fit between the two hydrographs is very close ($sd = 1.98$ mm/d, Fig. 4e). This
526 reflects the choice of the algorithm to mimic tracer baseflow separations (equations 7 and
527 8), which it does very well.

528

529 The three methods have been applied to hourly streamflow data for 1996. A sample of
530 each is shown for a two-week period in Figs. 4b, 4d and 4f. Only this short period is
531 shown because otherwise it is difficult to see the baseflow clearly. The parameters used
532 are listed in Table 2 along with the annual BFI values determined. The H & H baseflow
533 rises gradually through the stormflow peak, then follows the falling limb of the
534 streamflow after it intersects with it. The prescribed Eckhardt baseflow also rises

535 gradually through the peak then stays close to the recessing streamflow. The optimised
 536 Eckhardt baseflow rises sharply then falls sharply when it intersects the falling limb of
 537 the streamflow, and then gradually falls below the recessing streamflow curve. The BRM
 538 baseflow mirrors the streamflow peak then follows the falling streamflow after it
 539 intersects with it. It is also instructive to compare the BFI values derived by the various
 540 methods. The H & H method gives a BFI of 0.679, the Eckhardt methods BFIs of 0.617
 541 and 0.754 and the BRM method a BFI of 0.780 (almost the same as the Q_{90}/Q_{50} -derived
 542 BFI of 0.779, see this section below).

543
 544 Table 2 also shows estimates based on the characteristic flows from the flow duration
 545 curve (Q_{90}/Q_{50}). Smakhtin (2001) observed that the ratio of the two characteristic flows
 546 could be used to estimate BFI, and Collischonn and Fan (2013) derived equations
 547 connecting Q_{90}/Q_{50} and BFI_{max} and BFI based on results from fifteen catchments of
 548 varying sizes in Brazil. Their equations were

$$549 \quad 550 \quad BFI_{max} = 0.832 \frac{Q_{90}}{Q_{50}} + 0.216 \quad (20)$$

$$551 \quad 552 \quad BFI = 0.850 \frac{Q_{90}}{Q_{50}} + 0.163 \quad (21)$$

553
 554 These have been used to determine BFI_{max} and BFI in Table 2 (marked as FDC BFI_{max}
 555 and FDC BFI for clarity) for comparison with those derived using the three baseflow
 556 separation methods. There is a close correspondence between the FDC BFI and the BRM
 557 BFI, as noted, but the others are not particularly close. The backwards filter method of
 558 Collischonn and Fan (2013) has also been applied to estimate the BFI_{max} values for the
 559 prescribed and optimized Eckhardt parameters (Table 2). The resulting BFIs do not agree
 560 particularly well with the BFIs obtained from the other methods.

561
 562 The second way of determining the BRM parameters was described in the earlier version
 563 of this paper (Stewart, 2014a). Streamflow data was available for a summer month
 564 (February 1996) and a winter month (August 1996). These had different BFIs, but the
 565 bump fractions (f) obtained by finding the best-fits of the sum (i.e. baseflow plus fast
 566 recession) to the streamflow were similar at 0.16, while the slopes (k) were different. The
 567 fast recession was assumed to have a quadratic form (i.e. $d = 1.5$, equation 14) when
 568 fitting the sum to the streamflow, but the exponential ($d = 1$) and reciprocal ($d = 2$) forms
 569 were also tested and found to give the same quadratic result for the quickflow (i.e. slope
 570 of $d = 1.5$ on Fig. 5c) (Stewart 2014a). This optimizing process was also applied to the
 571 Eckhardt method in Stewart (2014b).

572 573 **3.2 Application of New Approach to Recession and Flow Duration Curve** 574 **Analysis**

575
 576 The recession behavior of the streamflow, BRM baseflow and BRM quickflow from the
 577 hourly streamflow record during 1996 are examined on recession plots (i.e. $-dQ/dt$ versus
 578 Q) in Figs. 5a-c. Discharge data less than two hours after rainfall has been excluded. The
 579 three figures have the same two lines on each. The first is a line through the lower part of
 580 the streamflow data with slope of 6 (this is called the streamflow line, see Fig. 5a). The
 581 second is a line through the quickflow points with slope of about 1.5 (this is called the
 582 quickflow line, see Fig. 5c). The streamflow points define a curve approaching the
 583 quickflow line at high flows when baseflow makes up only a small proportion of the

584 streamflow, and diverging from it when baseflow becomes more important. The slope of
585 a line through the points becomes much steeper in this lower portion (as shown by the
586 streamflow line), The baseflow points (Fig. 5b) have a similar pattern to the streamflow
587 points because the BRM baseflow shape mimics the streamflow shape at high to medium
588 flows because of the form of equations 7 & 8. At low flows the baseflow plots on the
589 streamflow and hence shows the same low flow pattern as the streamflow.

590

591 Quickflow is determined by subtracting baseflow from streamflow (Equation 1). It rises
592 rapidly from zero or near-zero at the onset of rainfall to a peak two to three hours after
593 rainfall, then falls back to zero in around 24 to 48 hours unless there is further rain. The
594 quickflow points at flows above about 1 mm/d fall on the quickflow line with slope of
595 1.5. Errors become much larger as quickflow becomes very small (i.e. as baseflow
596 approaches streamflow and quickflow is the small difference between the two). As Rupp
597 and Selker (2006) have noted “time derivatives of Q amplify noise and inaccuracies in
598 discharge data”. Nevertheless the quickflow points show a clear pattern supporting near-
599 quadratic fast recessions. The streamflow points might be expected to show a recession
600 slope of 1.5 at very low flows as the streamflow becomes dominated by baseflow, but the
601 data may not be accurate enough to show this (see Section 3.4).

602

603 Flow duration curves for streamflow, baseflow and quickflow are given in Fig. 5d. The
604 streamflow FDC has a very shallow slope indicating groundwater dominance over the
605 higher exceedance percentages. Streamflow diverges noticeably from baseflow below
606 about 17% exceedance (when quickflow reaches about 10% of streamflow). Note that the
607 temporal connection between the streamflow and components is not the same, each has
608 been sorted separately to produce the relevant FDC. The figure reveals the reasons for
609 breakpoints (i.e. changes of slope) in streamflow FDCs, which have been related to
610 contributions from different sources/reservoirs in catchments (e.g. Pfister et al., 2014).

611

612 **3.3 “Master” recession curve for Glendhu**

613

614 Fig. 6a shows the master recession curve not involving snowmelt or additional rainfall,
615 derived by Pearce et al. (1984) from the longest recessions observed during a three year
616 study period in GH1 and GH2 (before afforestation of GH2). The data for the curve come
617 from four storm events during winter and six during summer. These authors reported that
618 “This recession curve is typical of high to medium runoff events. The plot shows that
619 there is a marked change of slope between the early and late parts of the recessions (at a
620 flow of about 2.6 mm/d). Quickflow, as defined by the method of Hewlett and Hibbert
621 (1967), comprises 30% of the annual hydrograph and ceases shortly after the change in
622 recession rate in most hydrographs.”

623

624 The streamflow points from the master curve have been fitted by the sum of a quadratic
625 fast recession curve and the baseflow (Fig. 6b). The baseflow was calculated using the
626 parameters identified by the fitting to the pre-event hydrograph above ($f = 0.40$, $k = 0.009$
627 $\text{mm d}^{-1} \text{h}^{-1}$, Table 2). These parameters give a BFI of 0.828. During the late part of the
628 recession, when the baseflow dominates the streamflow, a slow recession curve was fitted
629 to the streamflow. The data are given in Table 2. The sum fits all of the points well and
630 there is a smooth transition between the early and late parts of the recession. The
631 inflexion point (Fig. 7b) occurs when the baseflow stops falling and begins to rise. The
632 inflexion point is therefore an expression of the change from the bump to the rise in the
633 baseflow and supports the BRM baseflow separation method. The change from early to

634 late recession when baseflow begins to dominate the recession comes considerably after
635 the inflexion point (Fig. 6b).

636

637 It is also instructive to see the recession plot of the data (Fig. 6c). The quickflow (i.e. fast)
638 and baseflow (i.e. slow) recessions are shown, both with slopes of 1.5. The early part of
639 the baseflow (i.e. the bump) is shown by the dashed curve. The sum of the fast recession
640 and the baseflow, which fits the streamflow points, is close to the fast recession at high
641 flow and matches the slow flow recession at low flows, as expected. The slope is steeper
642 at the medium flows between these two end states (the slope is about 6). This emphasises
643 the point that the slope of the streamflow points on a recession plot is meaningless in
644 terms of catchment storages at medium flows. Only the slopes of the quickflow and the
645 late-recession streamflow (which is the same as the late-recession baseflow) have
646 meaning in terms of storage types.

647

648 Fig. 6d shows the fraction of baseflow in the streamflow versus time according to the
649 tracer-based BRM. Baseflow makes up 32% of the streamflow at the highest flow, then
650 rises to 50% in about three hours (0.12 d), 75% at 14 hours (0.6 d) and 95% at 43 hours
651 (1.8 d). The change from early to late recession is shown at 1.8 d.

652

653

654 **4 Discussion**

655

656 **4.1 A new baseflow separation method: Advantages and limitations**

657

658 A new baseflow separation method (the BRM method) is presented. Advantages of the
659 method are:

660

661 (1) It aims to accurately simulate the shape of the baseflow or pre-event component
662 determined by tracers. This should mean that it gives more accurate baseflow separations
663 and BFIs, because tracer separation of the hydrograph is regarded as the only objective
664 method. The BRM method involves a rapid response to rainfall (the “bump”) and then a
665 gradual increase with time following rainfall (the “rise”).

666

667 (2) The parameters (f and k) quantifying the baseflow can be determined by fitting the
668 baseflow to tracer hydrograph separations (as illustrated in Section 3.2) or by fitting the
669 sum of the baseflow and a fast recession to the recession hydrograph under the constraint
670 of a BFI determined by flow considerations (as illustrated in Stewart, 2014a).

671

672 (3) The method can be applied using tracer data or streamflow data alone, and

673

674 (4) The method is easy to implement mathematically.

675

676 Current limitations or areas where further research may be needed are:

677

678 (1) Where there is no tracer data, specification of f and k depends on an initial estimate of
679 the BFI, although the optimisation procedure means that the precise value estimated for
680 the BFI is important, but not critical to the procedure.

681

682 (2) The method produces an averaged representation of the baseflow hydrograph when
683 applied to long-term data, so seasonal or intra catchment variations are likely.

684

685 (3) Separation of the hydrograph into three or more components (as shown by some
686 tracer studies) could be explored. The next section considers three components.

687

688 **4.2 Calibration of the BRM Algorithm**

689

690 This paper describes and demonstrates two ways of calibrating the BRM method (i.e.
691 determining its parameters f and k). These were also applied to the H & H and Eckhardt
692 methods. These are (1) fitting the methods to tracer separations, and (2) applying an
693 optimizing or other procedure. The tracer-based (first way) is demonstrated in this paper,
694 the optimizing procedure (second way) was demonstrated in the early (unreviewed)
695 version of this paper (Stewart, 2014a) and applied to the Eckhardt method in Stewart
696 (2014b). Additional procedures put forward by Collischon and Fan (2013), based on
697 characteristic flow duration curve flows (Q_{90}/Q_{50}) and a backwards filter, are also
698 compared with the other methods in this paper, but are not considered in detail.

699

700 Tracer separation of streamflow components depends on the tracer or tracers being used
701 and the experimental methods, etc. Klaus and McDonnell (2013) recently reviewed the
702 use of stable isotopes for hydrograph separation and restated the five underlying
703 assumptions. In the present case, deuterium was used by Bonell et al. (1990) to separate
704 the streamflow into event and pre-event components (Fig. 2a). The pre-event component
705 includes all of the water present in the catchment before the recorded rainfall event. The
706 pre-event component therefore includes soil water mobilized during the event as well as
707 groundwater. Three-component tracer separations have often been able to identify soil
708 water contributions along with direct precipitation and groundwater contributions in
709 streamflow (e.g. Iorgulescu et al. (2005) identified direct precipitation, acid soil and
710 groundwater components, Fig. 2b).

711

712 The second way of calibrating the BRM assumes a value for the BFI and then uses this as
713 a constraint to enable the sum (baseflow plus a fast recession) to be fitted to a streamflow
714 recession (winter and summer events were examined in Stewart, 2014a). It is assumed
715 that when the best-fit occurs (i.e. the baseflow has the optimum shape to fit to the
716 streamflow) that the baseflow shape will be most similar to the “true” groundwater shape.
717 The winter event BFI assumed is approximately in agreement with the BFIs given by the
718 H & H and prescribed Eckhardt methods when applied to the 1996 streamflow record
719 (the BFIs given by the H & H, prescribed Eckhardt and winter BRM methods are 0.679,
720 0.617 and 0.622 respectively). If this represents groundwater alone, then the difference
721 with the pre-event water (or the BRM baseflow matched to it) is the soil water component
722 as explained in Stewart (2014a). The groundwater and soil water components derived are
723 shown in Fig. 7 for the 23/2/88 event and two-week period in 1996. The soil water
724 component responds to rainfall more than the groundwater during events, then falls more
725 rapidly after them. In the absence of tracers, it is not generally possible to identify the
726 true groundwater component, but some BFI results appear to be “hydrologically more
727 plausible” than others (quoted phrase from Eckhardt, 2008). The BFI assumed for the
728 groundwater here is considered to be hydrologically plausible.

729

730 **4.3 Why is it necessary to apply baseflow separation to understand the** 731 **hydrograph?**

732

733 The answer is straightforward:

734

735 *Because streamflow is a mixture of quickflow and baseflow components, which have very*
736 *different characteristics and generation mechanisms and therefore give very misleading*
737 *results when analysed as a mixture.*

738

739 Previous authors (e.g. Hall, 1968, Brutsaert and Nieber, 1977, Tallaksen, 1995) addressed
740 “baseflow recession analysis” or “low flow recession analysis” in their titles, but
741 nevertheless included both early and late parts of the recession hydrograph in their
742 analyses. Kirchner (2009, P. 27) described his approach with the statement “the present
743 approach makes no distinction between baseflow and quickflow. Instead it treats
744 catchment drainage from baseflow to peak stormflow and back again, as a single
745 continuum of hydrological behavior. This eliminates the need to separate the hydrograph
746 into different components, and makes the analysis simple, general and portable”. This
747 work contends that catchment runoff is *not* a single continuum, and the varying
748 contributions of two or more very different components need to be kept in mind when the
749 power-law slopes of the points on recession plots are considered. Lack of separation has
750 probably led to misinterpretation of the slopes in terms of catchment storage reservoir
751 types.

752

753 Kirchner’s (2009) approach may be appropriate for his main purpose of “doing hydrology
754 backwards” (i.e. inferring rainfall from catchment runoff), but the current author suggests
755 that it gives misleading information about catchment storage reservoirs (as illustrated by
756 the different slopes of streamflow, quickflow and probably baseflow in Fig. 6c)). Note
757 also that Kirchner’s method is often used for recession analysis. Likewise Lamb and
758 Beven’s (1997) approach may have been fit-for-purpose for assessing the “catchment
759 saturated zone store”, but by combining parts of the early recession with the late
760 recession may give misleading information concerning catchment reservoir type (and
761 therefore catchment response). Others have used recession analysis on early and late
762 streamflow recessions for diagnostic tests of model structure at different scales (e.g.
763 Clark et al., 2009; McMillan et al., 2011) and it is suggested that these interpretations
764 may have produced misleading information on storage reservoirs.

765

766 Evidence of the very different characteristics and generation mechanisms of quickflow
767 and baseflow are provided by:

768

769 (1) The different timings of their releases to the stream (quick and slow) as shown by the
770 early and late parts of the recession curve. (Note: The rapid response of slow storage
771 water to rainfall (the “bump” in the BRM baseflow hydrograph) does not conflict with
772 this because the bump is due to celerity not to fast storage.)

773

774 (2) Many tracer studies (chemical and stable isotope) have shown differences between
775 quickflow and baseflow, and substantiated their different timings of storage.

776

777 (3) Transit times of streamwaters show great differences between quickflow and
778 baseflow. While quickflow is young (as shown by the variations of conservative tracers
779 and radioactive decay of tritium), baseflow can be much older with substantial fractions
780 of water having mean transit times beyond the reach of conservative tracer variations (4
781 years) and averaging 10 years as shown by tritium measurements (Stewart et al., 2010).

782

783 These considerations show that quickflow and baseflow are very different and in
784 particular have very different hydrographs, so their combined hydrograph (streamflow)
785 does not reflect catchment characteristics (except at low flows when there is no
786 quickflow).

787

788 **4.4 A new approach to recession analysis**

789

790 It appears that streamflow recession analysis is a technique in disarray (Stoelzle et al.,
791 2013). Different methods give different results and there is “a continued lack of
792 consensus on how to interpret the cloud of data points” (Brutsaert, 2005). This work
793 asserts that recession studies may have been giving misleading results in regard to
794 catchment functioning because streamflow is a varying mixture of components (unless
795 the studies were applied to late recessions only). The new approach of applying recession
796 analysis to the separated quickflow component as well as streamflow may help to resolve
797 this confusion, by demonstrating the underlying structure due to the different components
798 in recession plots (as illustrated in Fig. 6c). Plotting baseflow from the late part of the
799 recession may also be helpful. In particular, it is believed that recession analysis on
800 quickflow, and late recession baseflow as well as streamflow will give information that
801 actually pertains to those components, giving a clearer idea than before on the nature of
802 the water storages in the catchment, and contributing to broader goals such as catchment
803 characterisation, classification and regionalisation.

804

805 Observations from the data set in this paper and from some other catchments to be
806 reported elsewhere are:

807

808 (1) Quickflow appears to be quadratic in character (Section 7.2). This may result from a
809 variety of processes such as surface detention, passage through saturated zones within the
810 soil (perched zones) or within riparian zones near the stream. Whether this is true of
811 catchments in a wider variety of climatic regimes remains to be seen.

812

813 (2) The baseflow reservoirs at Glendhu appear to be quadratic in character, as has been
814 previously observed at many other catchments by other authors (Brutsaert and Nieber,
815 1977; Wittenberg, 1999; Dewandel, 2005; Stoelzle et al., 2013). Hillslope and valley
816 groundwater aquifers feed the water slowly to the stream.

817

818 (3) The many cases of high power-law slopes ($d > 1.5$) in recession plots reported in the
819 literature appear to be artifacts due to plotting early recession streamflow (particularly in
820 the intermediate flow range) instead of separated components. This may have also
821 contributed to the wide scatter of points generally observed in recession plots (referred to
822 as “high time variability in the recession curve” by Tallaksen, 1995).

823

824 (4) The most problematic parts of streamflow recession curves are those at intermediate
825 flows when quickflow and baseflow are approximately equal. This is where steep power-
826 law slopes are found. Data at high flows are dominated by quickflow, and baseflow
827 contributes almost all of the flow at low flows, so these parts do not have high power-law
828 slopes.

829

830 (5) Some other causes of scatter in recession plots are: insufficient accuracy of
831 measurements at low flows (Rupp and Selker, 2002), effects of rainfall during recession
832 periods (most data selection methods try to exclude these), different rates of

833 evapotranspiration in different seasons, different effects of rainfall falling in different
834 parts of the catchment, contributions from snowmelt or wetlands or deeper groundwater
835 systems, and drainage from different aquifers in different dryness conditions (McMillan
836 et al., 2011). These effects will be able to be examined more carefully when the
837 confounding effects of baseflow are removed from intermediate flows.

838
839 (6) Splitting the recession curve into early and late portions based on baseflow separation
840 turns out to be a very useful thing to do. The early part has quickflow plus the
841 confounding effects of baseflow, while the late part has only baseflow. The late part starts
842 when baseflow becomes predominant (>95%, Fig. 6d), this can be calculated by
843 identifying the point where $B_t/Q_t = 0.95$ during a recession. It appears that at Glendhu,
844 the inflexion point records a change of slope *in the baseflow* and lies within the early part
845 of the recession.

846
847 (7) The close links between surface water hydrology and groundwater hydrology are
848 revealed as being even closer by this work. Baseflow is mostly groundwater, and
849 quickflow is also starting to look distinctly groundwater-influenced (or saturation-
850 influenced). The success of groundwater models (Gusyev et al., 2013, 2014) in
851 simulating tritium concentrations and baseflows in streams while being calibrated to
852 groundwater levels in wells shows the intimate connection between the two. The feeling
853 that catchment drainage can be treated as a single continuum of hydrological behavior has
854 probably prevented recognition of the disparate natures of the quick and slow drainages.
855 This may be a symptom of the fact that surface water hydrology and groundwater
856 hydrology can be regarded as different disciplines (Barthel, 2014). Others however are
857 crossing the divide by examining geological controls on BFIs (Bloomfield et al., 2009)
858 and relating baseflow simulation to aquifer model structure (Stoelzle et al., 2014).

861 **5 Conclusions**

862
863 This paper has two main messages. The first is the introduction of a new baseflow
864 separation method (the bump and rise method or BRM). The advantage of the BRM is
865 that it specifically simulates the shape of the baseflow or pre-event component as shown
866 by tracers. Tracer separations are regarded as the only objective way of determining
867 baseflow separations and BFIs, so the BRM method should give relatively more accurate
868 baseflow separations and BFIs. The BRM parameters are determined by either fitting
869 them to tracer separations (which are usually determined on a small number of events) as
870 illustrated in this paper, or by estimating the BFI and using it as a constraint which
871 enables determination of the BRM parameters by an optimization procedure on an event
872 or events as illustrated in an earlier version of this paper (Stewart, 2014a). The BRM
873 algorithm can then be simply applied to the entire streamflow record.

874
875 Current limitations or areas where further research could be needed are: (1) specification
876 of f and k depends on tracer information or an initial estimate of the BFI, although the
877 optimisation procedure means that the precise value estimated for the BFI is important
878 but not critical to the procedure, (2) the method applied to long-term data produces an
879 averaged representation of the baseflow hydrograph, so seasonal or intra catchment
880 variations are likely, and (3) separation of the hydrograph into three components (as
881 shown by some tracer studies) could be explored (and has been for the Glendhu
882 Catchment).

883

884 The second main message is that recession analysis of streamflow alone on recession
885 plots can give very misleading results regarding the nature of catchment storages because
886 streamflow is a varying mixture of components. Instead, plotting separated quickflow
887 gives insight into the early recession flow sources (high to intermediate flows), and
888 separated baseflow (which is equal to streamflow) gives insight into the late recession
889 flow sources (low flows). The very different behaviours of quickflow and baseflow are
890 evident from their different timings of release from storage (shown by the early and late
891 portions of the recession curve, by tracer studies, and by their very different transit
892 times). Clearer ideas on the nature of the storages in the catchment can contribute to
893 broader goals such as catchment characterisation, classification and regionalization, as
894 well as modelling. Flow duration curves can also be determined for the separated stream
895 components, and these help to illuminate the makeup of the streamflow at different
896 exceedance percentages.

897

898 Conclusions drawn from applying recession analysis to separated components in this
899 paper are: (1) Many cases of high power-law slopes ($d > 1.5$) in recession plots reported in
900 the literature are likely to be artifacts due to plotting early recession streamflow instead of
901 quickflow. The most problematic parts of streamflow recession curves are those at
902 intermediate flows when quickflow and baseflow are approximately equal. This is where
903 steep power-law slopes are found. (2) Both quickflow and baseflow reservoirs appear to
904 be quadratic in character, suggesting that much streamwater passes through saturated
905 zones (perched zones in the soil, riparian zones, groundwater aquifers) at some stage. (3)
906 Other causes of scatter in recession plots will be able to be examined more carefully
907 when the confounding effects of baseflow are removed from intermediate flows. (4)
908 Splitting the recession curve into early and late portions is very informative, because of
909 their different makeups. The late part starts when baseflow becomes predominant.

910

911 Some suggestions for the way forward in light of the findings of this paper are: (1)
912 Recession analyses (and transit time analyses and chemical/discharge relationships)
913 should be qualified with the component being analysed. This will make the significance
914 of the results clearer. (2) Rainfall-runoff models should make more use of (non-linear)
915 quadratic storage systems for simulating streamflow. (3) Much more data on many other
916 catchment areas needs to be examined in this way to develop and refine these concepts.

917

918

919 **6 Acknowledgements**

920

921 I thank Barry Fahey, John Payne and staff of Landcare Research NZL for data and
922 cooperation on Glendhu Catchment studies.

923

924 **7 References**

925

926 Bazemore, D. E., Eshleman, K. N. and Hollenbeck, K. J.: The role of soil water in
927 stormflow generation in a forested headwater catchment: synthesis of natural
928 tracer and hydrometric evidence, *J. Hydrol.*, 162, 47-75, 1994.

929 Barthel, R.: HESS Opinions "Integration of groundwater and surface water research: an
930 interdisciplinary problem?", *Hydrol. Earth Syst. Sci.*, 18, 2615-2628, 2014.

931 Beven, K. J.: Hydrograph separation? In *Proceedings of the BHS 3rd National Hydrology
932 Symposium*, Southampton, 1991.

933 Beven, K. J.: Rainfall-runoff modelling: the primer, 2nd ed. Wiley-Blackwell, Chichester.
934 2012.

935 Biswal, B. and Marani M.: Geomorphological origin of recession curves. *Geophys. Res.*
936 *Lett.*, 37: L24403, 2010.

937 Bloomfield, J. P., Allen, D. J. and Griffiths K. J.: Examining geological controls on
938 baseflow index (BFI) using regression analysis: An illustration from the Thames
939 Basin, UK, *J. Hydrol.*, 373 (1–2), 164-176, 2009.
940 doi:10.1016/j.jhydrol.2009.04.025

941 Bonell, M., Pearce, A. J. and Stewart M. K.: Identification of runoff production
942 mechanisms using environmental isotopes in a tussock grassland catchment,
943 Eastern Otago, New Zealand, *Hydrol. Processes*, 4(1), 15-34, 1990.

944 Boussinesq, J.: Essai sur la théorie des eaux courantes, *Memoires de l'Académie des*
945 *Sciences de l'Institut de France*, 23, 252–260, 1877.

946 Boussinesq, J.: Sur un mode simple d'écoulement des nappes d'eau d'infiltration à lit
947 horizontal, avec rebord vertical tout autour lorsqu'une partie de ce rebord est
948 enlevée depuis la surface jusqu'au fond, *C. R. Acad. Sci.*, 137, 5–11, 1903.

949 Bowden, W. B., Fahey, B. D., Ekanayake, J. and Murray, D. L.: Hillslope and wetland
950 hydrodynamics in a tussock grassland, Southland, New Zealand, *Hydrol.*
951 *Processes*, 15, 1707–1730, 2001.

952 Brutsaert, W. and Nieber J. L.: Regionalized drought flow hydrographs from a mature
953 glaciated plateau, *Water Resour. Res.*, 13(3), 637-643, 1977.

954 Brutsaert, W.: *Hydrology: An Introduction*, Cambridge University Press, Cambridge,
955 UK, 605 pp., 2005.

956 Buttle, J. M.: Isotope hydrograph separations and rapid delivery of pre-event water from
957 drainage basins, *Prog. Phys. Geog.*, 18, 16-41, 1994.

958 Campbell, D. I., and Murray, D. L.: Water balance of snow tussock grassland in New
959 Zealand. *J. Hydrol.*, 118, 229-245, 1990.

960 Chapman, T. G.: A comparison of algorithms for streamflow recession and baseflow
961 separation, *Hydrol. Processes*, 13, 701-714, 1999.

962 Chapman, T. G. and Maxwell A. I.: Baseflow separation - Comparison of numerical
963 methods with tracer experiments, In *Proceedings of the 23rd Hydrology and Water*
964 *Resources Symposium*. Hobart, Australia, 539-545, 1996.

965 Clark, M. P., Rupp, D. E., Woods, R. A., Tromp-van Meerveld, H. J., Peters, N. E. and
966 Freer J. E.: Consistency between hydrological models and field observations:
967 linking processes at the hillslope scale to hydrological responses at the watershed
968 scale, *Hydrol. Process.*, 33, 311-319, 2009.

969 Collischon, W. and Fan, F. M.: Defining parameters for Eckhardt's digital baseflow filter.
970 *Hydrol. Process.* 27, 2614-2622. DOI: 10.1002/hyp.9391, 2013.

971 Dewandel, B., Lachassagne, P., Bakalowicz, M., Weng, P. and Al-Malki, A.: Evaluation
972 of aquifer thickness by analysing recession hydrographs. Application to the Oman
973 ophiolite hard-rock aquifer, *J. Hydrol.*, 274, 248-269, 2003.

974 Eckhardt, K.: How to construct recursive digital filters for baseflow separation, *Hydrol.*
975 *Process.*, 19, 507–515. DOI: 10.1002/hyp.5675, 2005.

976 Eckhardt, K.: A comparison of baseflow indices, which were calculated with seven
977 different baseflow separation methods, *J. Hydrol.*, 352, 168-173, 2008.

978 Fahey, B. D., and Jackson, R. J.: Hydrological impacts of converting native forest and
979 grasslands to pine plantations, South Island, New Zealand, *Agric. Forest*
980 *Meteorol.*, 84, 69–82, 1997.

- 981 Fenicia, F., Kavetski, D. and Savenije H. H. G.: Elements of a flexible approach for
982 conceptual hydrological modelling: 1. Motivation and theoretical development,
983 *Water Resour. Res.*, 47, W11510, doi:10.1029/2010WR010174, 2011.
- 984 Fenicia, F., Savenije, H. H. G., Matgen, P. and Pfister, L.: Is the groundwater reservoir
985 linear? Learning from data in hydrological modeling, *Hydrol. Earth Syst. Sci.*,
986 10(1), 139-150, 2006.
- 987 Gonzales, A. L., Nonner, J., Heijers, J. and Uhlenbrook, S.: Comparison of different
988 baseflow separation methods in a lowland catchment, *Hydrol. Earth Syst. Sci.*, 13,
989 2055-2068, 2009.
- 990 Gusyev, M. A., Abrams, D., Toews, M. W., Morgenstern, U., Stewart, M. K.: A
991 comparison of particle-tracking and solute transport methods for
992 simulation of tritium concentrations and groundwater transit times in river
993 water. *Hydrol. Earth Syst. Sci.*, 18, 3109-3119. 2014. doi:10.5194/hess-18-
994 3109-2014
- 995 Gusyev, M.A., Toews, M. W., Morgenstern, U., Stewart, M. K. and Hadfield, J.:
996 Calibration of a transient transport model to tritium measurements in rivers and
997 streams in the western Lake Taupo catchment, New Zealand, *Hydrol. Earth Syst.*
998 *Sci.*, 17, 1217-1227, 2013.
- 999 Hall, F. R.: Base-flow recessions – A review, *Water Resour. Res.*, 4, 975-983, 1968.
- 1000 Hangen, E., Lindenlaub, M., Leibundgut, Ch. and von Wilpert, K.: Investigating
1001 mechanisms of stormflow generation by natural tracers and hydrometric data: a
1002 small catchment study in the Black Forest, Germany, *Hydrol. Processes*, 15, 183-
1003 199, 2001.
- 1004 Hewlett, J.D. and Hibbert, A. R.: Factors affecting the response of small watersheds to
1005 precipitation in humid areas, in *Forest Hydrology*, edited by W. E. Sopper and H.
1006 W. Lull, pp. 275–290, Pergamon, Oxford, 1967.
- 1007 Hrachowitz, M., Savenije, H., Bogaard, H., Tetzlaff, D. and Soulsby C.: What can flux
1008 tracking teach us about water age distributions and their temporal dynamics?
1009 *Hydrol. Earth Syst. Sci.*, 17, 533-564, 2013.
- 1010 Holko, L., Herrmann, A., Uhlenbrook, S., Pfister, L. and Querner E.: Ground water
1011 runoff separation – test of applicability of a simple separation method under
1012 varying natural conditions, *Friend 2002 – Regional hydrology: Bridging the gap*
1013 *between research and practice (IAHS Publication no. 274)*, 265-272, 2002.
- 1014 Hooper, R.P. and Shoemaker, C. A.: A comparison of chemical and isotopic hydrograph
1015 separation, *Water Resour. Res.*, 22, 1444-1454, 1986.
- 1016 Iorgulescu, I., Beven, K. J. and Musy, A.: Data-based modelling of runoff and chemical
1017 tracer concentrations in the Haute-Mentue research catchment (Switzerland),
1018 *Hydrol. Processes*, 19, 2557-2573, 2005.
- 1019 Iwagami, S., Tsujimura, M., Onda, Y., Shimada, J. and Tanaka T.: Role of bedrock
1020 groundwater in the rainfall–runoff process in a small headwater catchment
1021 underlain by volcanic rock, *Hydrol. Processes*, 24, 2771-2783. DOI:
1022 10.1002/hyp.7690, 2010.
- 1023 Joerin, C., Beven, K. J., Iorgulescu, I. and Musy A.: Uncertainty in hydrograph
1024 separations based on mixing models. *J. Hydrol.*, 255, 90-106, 2002.
- 1025 Kirchner, J. W.: Catchments as simple dynamical systems: Catchment characterization,
1026 rainfall-runoff modelling, and doing hydrology backward, *Water Resour. Res.*,
1027 45:W02429, doi:10.1029/2008WR006912, 2009.
- 1028 Klaus, J. and McDonnell, J. J.: Hydrograph separation using stable isotopes: Review and
1029 evaluation, *J. Hydrol.*, 505, 47-64, 2013.

1030 Lamb, R. and Beven, K. J.: Using interactive recession curve analysis to specify a general
1031 catchment storage model, *Hydrol. Earth Syst. Sci.*, 1, 101-103, 1997.

1032 Linsley, R. K., Kohler, M. A. and Paulhus, J. L.: *Hydrology for Engineers*, McGraw-Hill,
1033 New York, 1975.

1034 Lyne, V. D., Hollick, M. Stochastic time-variable rainfall runoff modelling. *Hydrology
1035 and Water Resources Symposium*, Institution of Engineers Australia, Perth. 89-
1036 92, 1979.

1037 McDonnell, J. J., Beven, K. J.: Debates – The future of Hydrological Sciences: A
1038 (common) path forward? A call to action aimed at understanding velocities,
1039 clerities and residence time distributions of the headwater hydrograph, *Water
1040 Resour. Res.*, 80, 5342-5350, 2014. Doi:10.1002/2013WR015141.

1041 McDonnell, J. J., Bonell, M., Stewart, M. K. and Pearce, A. J.: Deuterium variations in
1042 storm rainfall – Implications for stream hydrograph separation, *Water Resour.
1043 Res.*, 26, 455-458, 1991.

1044 McMillan, H. K., Clark, M. P., Bowden, W. B., Duncan, M. and Woods, R.:
1045 Hydrological field data from a modeller's perspective: Part 1. Diagnostic tests for
1046 model structure, *Hydrol. Process.* 25, 511-522, 2011.

1047 Michel, R. L., Aggarwal, P., Araguas-Araguas, L., Kurttas, T., Newman, B. D. and
1048 Vitvar, T.: A simplified approach to analyzing historical and recent tritium data in
1049 surface waters, *Hydrol. Processes*, DOI: 10.1002/hyp. 10174, 2014.

1050 Nejadhashemi, A. P., Shirmohammadi, A. and Montas, H. J.: Evaluation of streamflow
1051 partitioning methods, Pap. No. 032183 in ASAE Annual International Meeting,
1052 edited by M. St. Joseph M, Las Vegas, Nevada, USA, 2003.

1053 Pearce, A. J., Rowe, L. K. and O'Loughlin, C. L.: Hydrology of mid-altitude tussock
1054 grasslands, upper Waipori catchment, Otago: II Water balance, flow duration and
1055 storm runoff, *J. Hydrol. (NZ)*, 23, 60-72, 1984.

1056 Pfister, L., McDonnell, J. J., Hissler, Ch., Klaus, J., Stewart M. K.: Geological controls
1057 on catchment mixing, storage, and release. *Hydrol. Process.*, in review, 2014.

1058 Pinder, G. F. and Jones, J. F.: Determination of the ground-water component of peak
1059 discharge from the chemistry of total runoff. *Water Resour. Res.*, 5, 438-445.
1060 DOI:10.1029/WR005i002p00438, 1969.

1061 Rupp, D. E. and Selker, J. S.: Information, artifacts and noise in $dQ/dt - Q$ recession
1062 analysis, *Adv. Water Resour.*, 29, 154-160, 2006.

1063 Searcy, R. K.: Flow-duration curves, *Manual of Hydrology: Part 2. Low-flow techniques*,
1064 Geological Survey Water-Supply paper 1542-A, 33 p, 1959.

1065 Shaw, S. B. and Riha, J. S.: Examining individual recession events instead of a data
1066 cloud: Using a modified interpretation of $dQ/dt-Q$ streamflow recession in
1067 glaciated watersheds to better inform models of low flow, *J. Hydrol.*, 434-435, 46-
1068 54, 2012.

1069 Sklash, M. G. and Farvolden, R. N.: The role of groundwater in storm runoff, *J. Hydrol.*,
1070 43, 45-65, 1979.

1071 Sloto, R. A. and Crouse, M. Y.: HYSEP: A computer program for streamflow hydrograph
1072 separation and analysis, US Geological Survey, Water-Resources Investigations
1073 Report 96-4040, 1996.

1074 Smakhtin, V. U.: Low flow hydrology: A review, *J. Hydrol.*, 240, 147-186, 2001.

1075 Stewart, M. K.: New baseflow separation and recession analysis approaches for
1076 streamflow. *Hydrol. Earth Syst. Sci., Discuss.*, 11, 7089-7131, 2014a.
1077 doi:10.5194/hessd-11-7089-2014

1078 Stewart, M. K.: Interactive comment on “New baseflow separation and recession analysis
1079 approaches for streamflow” by M. K. Stewart, *Hydrol. Earth Syst. Sci. Discuss.*,
1080 11, C3964-C3964, 2014b.

1081 Stewart, M. K. and Fahey, B. D.: Runoff generating processes in adjacent tussock
1082 grassland and pine plantation catchments as indicated by mean transit time
1083 estimation using tritium, *Hydrol. Earth Syst. Sci.*, 14, 1021-1032, 2010.

1084 Stewart, M.K., Mehlhorn, J. and Elliott, S.: Hydrometric and natural tracer (^{18}O , silica, ^3H
1085 and SF_6) evidence for a dominant groundwater contribution to Pukemanga
1086 Stream, New Zealand, *Hydrol. Processes*, 21(24), 3340-3356.
1087 DOI:10.1002/hyp.6557, 2007.

1088 Stewart, M. K., Morgenstern, U. and McDonnell, J. J.: Truncation of stream residence
1089 time: How the use of stable isotopes has skewed our concept of streamwater age
1090 and origin, *Hydrol. Processes*, 24(12), 1646-1659, 2010.

1091 Stewart, M. K., Morgenstern, U., McDonnell, J. J. and Pfister, L.: The “hidden
1092 streamflow” challenge in catchment hydrology: A call to action for
1093 streamwater transit time analysis, *Hydrol. Processes* 26(13), 2061-2066.
1094 doi: 10.1002/hyp.9262, 2012.

1095 Stoelzle, M., Stahl, K. and Weiler, M.: Are streamflow recession characteristics really
1096 characteristic? *Hydrol. Earth Syst. Sci.*, 17, 817–828, 2013.

1097 Stoelzle, M., Weiler, M., Stahl, K., Morhard, A. and Schuetz, T.: Is there a superior
1098 conceptual groundwater model structure for baseflow simulation?, *Hydrol.*
1099 *Process.* 2014. DOI: 10.1002/hyp.10251

1100 Su, N. G.: The Unit-Hydrograph Model for Hydrograph Separation, *Environ. Internat.*,
1101 21, 509–515, 1995.

1102 Tallaksen, L.M.: A review of baseflow recession analysis, *J. Hydrol.*, 165, 349-370,
1103 1995.

1104 Vogel, R. and Kroll, C.: Regional geohydrogeologic-geomorphic relationships for the
1105 estimation of low-flow statistics, *Water Resour. Res.*, 28, 2451-2458, 1992.

1106 Westerberg, I. K., Guerrero, J.-L., Younger, P. M., Beven, K. J., Seibert, J., Halldin, S.,
1107 Freer, J. E. and Xu, C.-Y.: Calibration of hydrological models using flow-duration
1108 curves, *Hydrol. Earth Syst. Sci.*, 15, 2205-2227, 2011.

1109 Wittenberg, H.: Baseflow recession and recharge as nonlinear storage processes, *Hydrol.*
1110 *Processes*, 13, 715-726, 1999.

1111 Zhang, R., Li, Q., Chow, T. L., Li, S. and Danielescu, S.: Baseflow separation in a small
1112 watershed in New Brunswick, Canada, using a recursive digital filter calibrated
1113 with the conductivity mass balance method, *Hydrol. Processes*, 27, 2659-2665,
1114 2013.

1115

1116

1117 Table 1. Tracer calibration of the baseflow separation methods by comparison with pre-
 1118 event water determined using deuterium for a streamflow event on 23 February 1988 at
 1119 Glendhu GH1 Catchment (Bonell et al., 1990). The listed parameters were determined as
 1120 described in the text. The standard deviations (sd) show the goodness of fit between the
 1121 various baseflows and the pre-event water.

Separation Method	BFI ^a	f ^a	k ^a mmd ⁻¹ h ⁻¹	BFI _{max} ^a	a ^a h ⁻¹	sd mmd ⁻¹
Pre-event water	0.529	--	--	--	--	--
H & H	0.255	--	0.0472	--	--	6.41
Eckhardt (prescribed)	0.272	--	--	0.8	0.9982	6.34
Eckhardt (optimised)	0.524	--	--	0.886	0.991	5.40
BRM	0.526	0.4	0.009	--	--	1.98

1122 ^aBFI is baseflow index, f bump fraction, k slope parameter, BFI_{max} maximum value of the
 1123 baseflow index that can be modelled by the Eckhardt algorithm, and a recession constant.
 1124
 1125
 1126
 1127
 1128

1129 Table 2. BFIs and parameters of the baseflow separation methods applied to the hourly
 1130 streamflow record in 1996, and to the master recession curve. The Q_{90}/Q_{50} ratio is from
 1131 the flow duration curve for 1996, and the FDC BFI_{max} and FDC BFI are from equations
 1132 20 and 21 in the text.

Separation Method	BFI ^a	f ^a	k ^a mmd ⁻¹ h ⁻¹	BFI _{max} ^a	a ^a h ⁻¹
Q_{90}/Q_{50}	0.728	--	--	--	--
FDC BFI_{max} (eqn 20)	--	--	--	0.824	--
FDC BFI (eqn 21)	0.779	--	--	--	--
H & H	0.679	--	0.0472	--	--
Eckhardt (prescribed)	0.617	--	--	0.8	0.9982
Eckhardt (back filter)	0.521	--	--	0.593	0.9982
Eckhardt (optimised)	0.754	--	--	0.886	0.991
Eckhardt (back filter)	0.580	--	--	0.668	0.991
BRM	0.780	0.4	0.009	--	--
Master recession curve	0.828	0.4	0.009	--	--

1133 ^aBFI is baseflow index, f bump fraction, k slope parameter, BFI_{max} maximum value of the
 1134 baseflow index that can be modelled by the Eckhardt algorithm, and a recession constant.
 1135

1136 **Figure Captions**

1137

1138 Figure 1 Quickflow and baseflow components of streamflow, and the early and late parts
1139 of the recession curve. Quickflow is represented by the area between the streamflow and
1140 baseflow curves, and baseflow is the area under the baseflow curve.

1141

1142 Figure 2 Tracer hydrograph separation results. (a) Event/pre-event water separation from
1143 catchment GH1, Glendhu, New Zealand using deuterium (replotted from Bonell et al.,
1144 1990). (b) Three component separation from Haute-Mentue research catchment,
1145 Switzerland using silica and calcium (replotted from Iorgulescu et al., 2005). R/F is
1146 rainfall, SF streamflow and the flow components are DP direct precipitation, AS acid soil
1147 and GW groundwater.

1148

1149 Figure 3 Map of Glendhu catchments (GH1 and GH2). The inset shows their location in
1150 the South Island of New Zealand.

1151

1152 Figure 4 (a, c, e) Application of the three baseflow separation methods to fit the pre-event
1153 component determined by deuterium measurements at Glendhu GH1 Catchment for an
1154 event on 23/2/88. The parameters determined by fitting are given in Table 2. (b, d, f)
1155 Baseflows resulting from the best-fit parameters for a two-week period in 1996. Note the
1156 logarithmic scales.

1157

1158 Figure 5. (a-c) Recession plots showing streamflow, baseflow and quickflow from the
1159 1996 GH1 hourly flow record. The line through the mid-flow streamflow and baseflow
1160 points has slope of 6.0, and that through the higher flow quickflow points (flows greater
1161 than 1 mm/d) has slope of 1.5. (d) Flow duration curve showing streamflow, baseflow
1162 and quickflow.

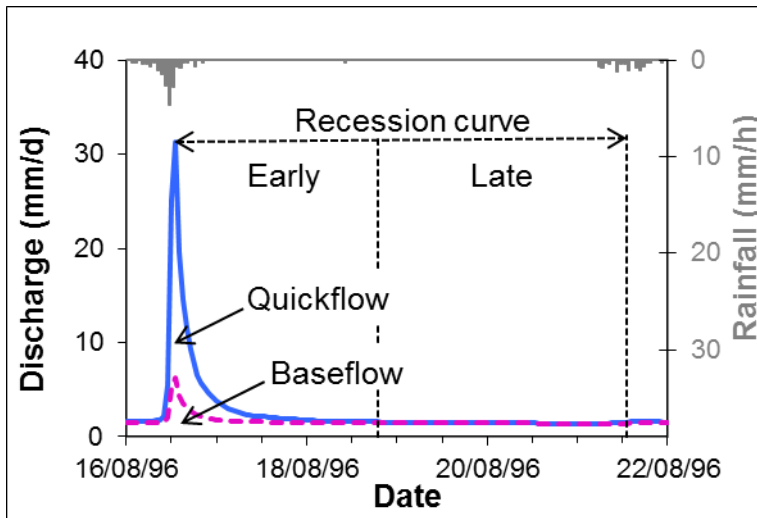
1163

1164 Figure 6. (a) "Master" recession curve for Glendhu GH1 catchment (redrawn from Pearce
1165 et al., 1984). (b) Master recession data matched by the sum of the baseflow and a fast
1166 recession curve. The arrow shows the inflexion point. Early and late parts of the master
1167 recession curve are shown. (c) Recession plot of master recession curve (sum), baseflow
1168 and fast recession. The sum is close to the fast recession curve at high flows and close to
1169 the baseflow (slow recession curve) at low flows. The dashed part of the curve shows the
1170 "bump" in the baseflow. (d) Variation of the baseflow contribution to streamflow with
1171 time during the master recession curve.

1172

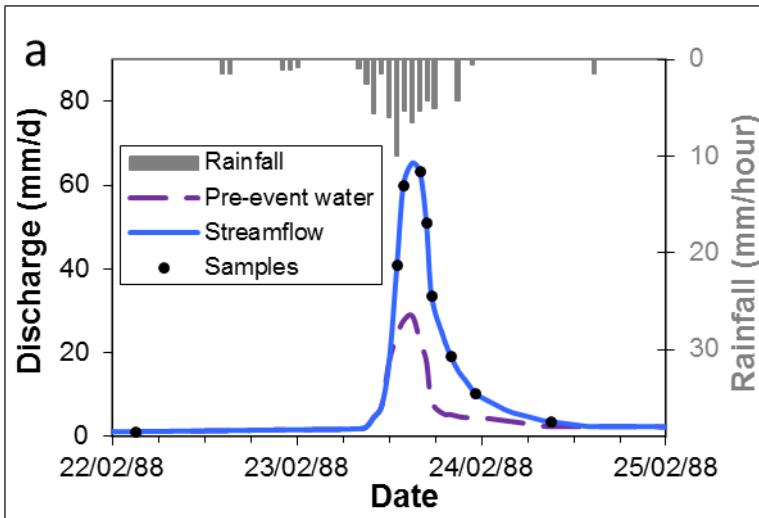
1173 Figure 7 (a, b) Plots showing groundwater and soil water components of the baseflow
1174 matched to the pre-event hydrograph. Streamflow is pre-event water plus event water.

1175

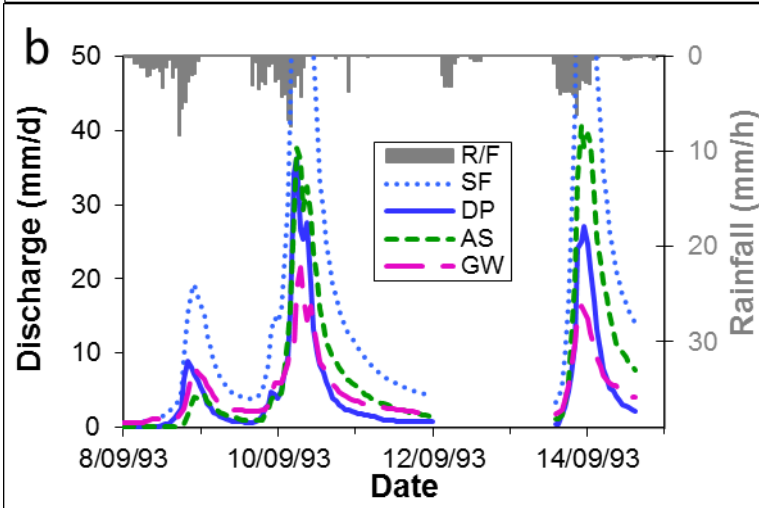


1176

1177 Figure 1 Quickflow and baseflow components of streamflow, and the early and late parts
 1178 of the recession curve. Quickflow is represented by the area between the streamflow and
 1179 baseflow curves, and baseflow is the area under the baseflow curve.
 1180



1181

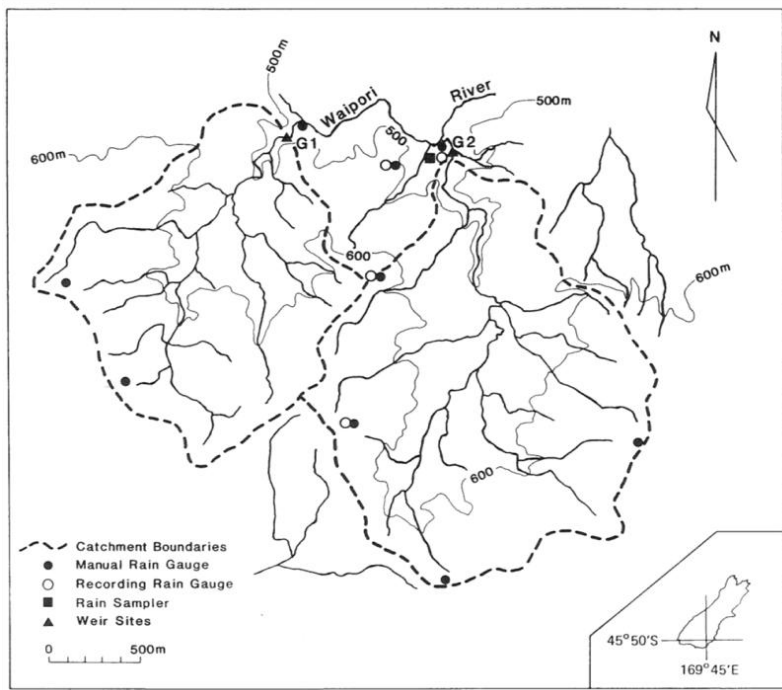


1182

1183

1184 Figure 2 Tracer hydrograph separation results. (a) Event/pre-event water separation from
 1185 catchment GH1, Glendhu, New Zealand using deuterium (replotted from Bonell et al.,
 1186 1990). (b) Three component separation from Haute-Mentue research catchment,
 1187 Switzerland, using silica and calcium (replotted from Iorgulescu et al., 2005). R/F is
 1188 rainfall, SF streamflow and the flow components are DP direct precipitation, AS acid soil
 1189 and GW groundwater

1190

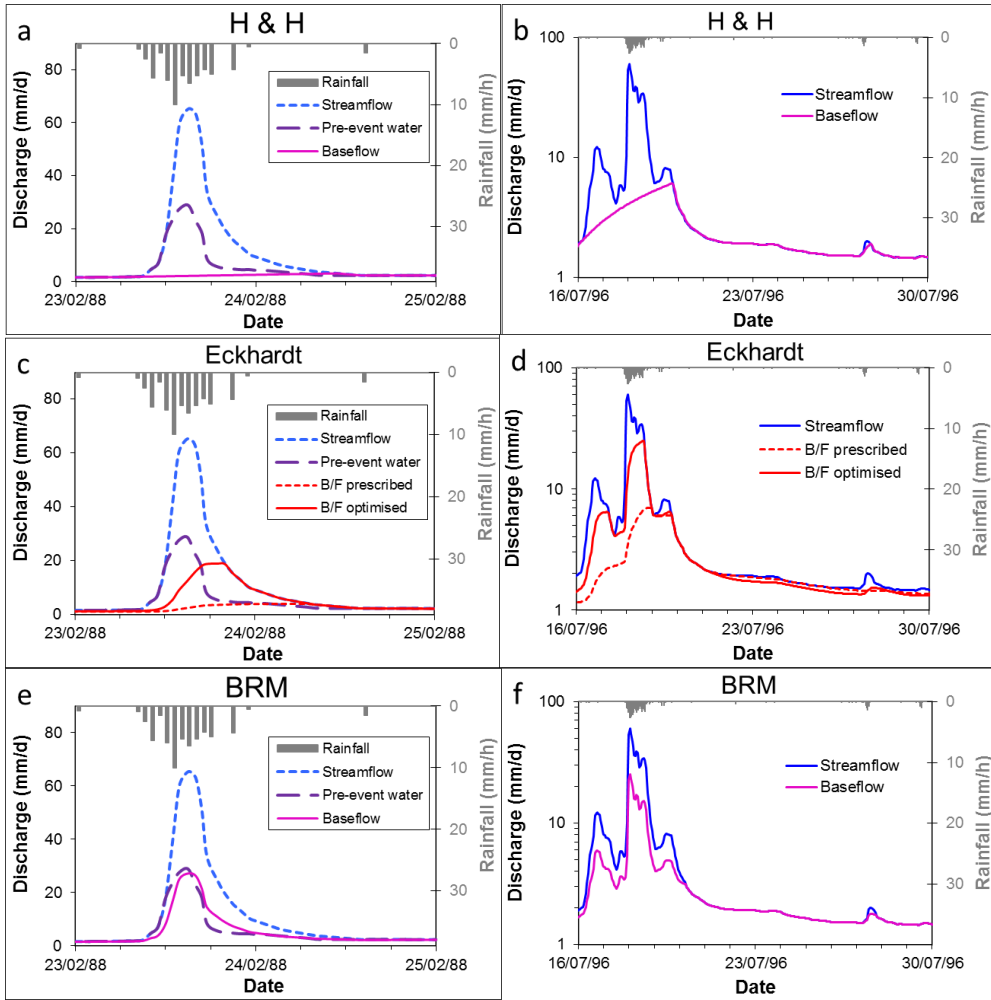


1191

1192 Figure 3 Map of Glendhu catchments (GH1 and GH2). The inset shows their location in
 1193 the South Island of New Zealand.

1194

1195



1196

1197

1198

1199

1200

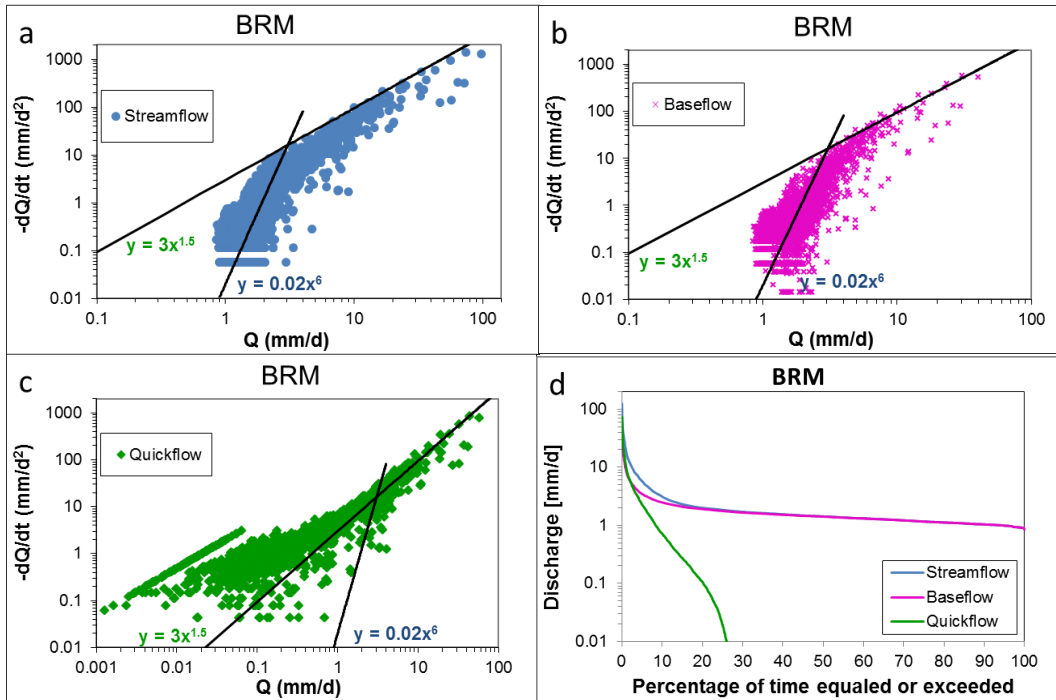
1201

1202

1203

Figure 4 (a, c, e) Fits of the three baseflow separation methods to pre-event water determined by deuterium measurements at Glendhu GH1 Catchment for an event on 23/2/88. The parameters determined by fitting are given in Table 1. (b, d, f) Baseflows resulting from the best-fit parameters for a two-week period in 1996. Note the logarithmic vertical scales.

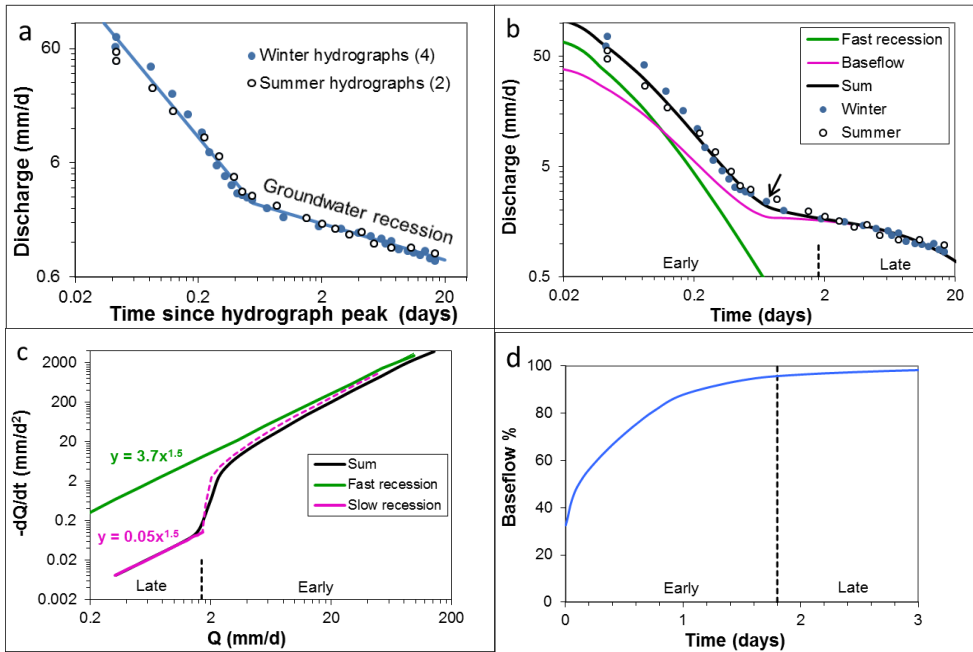
1204



1205
1206
1207
1208
1209
1210
1211
1212

Figure 5 (a-c) Recession plots showing streamflow, baseflow and quickflow from the 1996 GH1 flow record using the BRM method. The line through the mid-flow streamflow and baseflow points has slope of 6.0, and that through the higher flow quickflow points (flows greater than 1 mm/d) has slope of 1.5. Note the wider range of the horizontal axis in (c). (d) Flow duration curve showing streamflow, baseflow and quickflow.

1213



1214

1215

1216

1217

1218

1219

1220

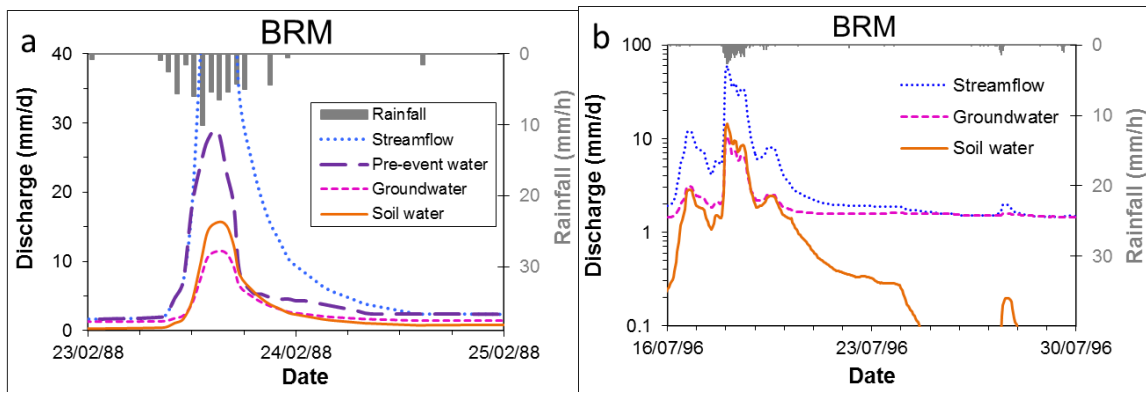
1221

1222

1223

Figure 6 (a) “Master” recession curve for Glendhu GH1 catchment (redrawn from Pearce et al., 1984). (b) Master recession data matched by the sum of the BRM baseflow and fast recession curve. The arrow shows the inflexion point. Early and late parts of the master recession curve are shown. (c) Recession plot of master recession curve (sum), baseflow and fast recession. The sum is close to the fast recession curve at high flows and close to the baseflow (slow recession curve) at low flows. The dashed curve shows the “bump” in the baseflow. (d) Variation of the baseflow contribution to streamflow with time during the master recession curve.

1224



1225

1226

1227

1228

Figure 7 (a, b) Plots showing groundwater and soil water components of the baseflow matched to the pre-event hydrograph. Streamflow is pre-event water plus event water.